

Pyrrolizine-5-carboxamides: Exploring the impact of various substituents on anti-inflammatory and anticancer activities

AHMED M. GOUDA^{1,2*}
AHMED H. ABDELAZEEM²
ASHRAF N. ABDALLA^{3,4}
MUHAMMAD AHMED³

¹ Department of Pharmaceutical Chemistry, Faculty of Pharmacy Umm Al-Qura University, Makkah 21955, Saudi Arabia

² Department of Medicinal Chemistry, Faculty of Pharmacy Beni-Suef University, Beni-Suef 62514, Egypt

³ Department of Pharmacology and Toxicology, Faculty of Pharmacy Umm Al-Qura University, Makkah 21955, Saudi Arabia

⁴ Department of Pharmacology Medicinal and Aromatic Plants Research Institute National Center for Research Khartoum 2404, Sudan

Towards optimization of the pyrrolizine-5-carboxamide scaffold, a novel series of six derivatives (**4a-c** and **5a-c**) was prepared and evaluated for their anti-inflammatory, analgesic and anticancer activities. The (*EZ*)-7-cyano-6-((4-hydroxybenzylidene)amino)-*N*-(*p*-tolyl)-2,3-dihydro-1*H*-pyrrolizine-5-carboxamide (**4b**) and (*EZ*)-6-((4-chlorobenzylidene)-amino)-7-cyano-*N*-(*p*-tolyl)-2,3-dihydro-1*H*-pyrrolizine-5-carboxamide (**5b**) bearing the electron donating methyl group showed the highest anti-inflammatory activity while (*EZ*)-6-((4-chlorobenzylidene)amino)-7-cyano-*N*-phenyl-2,3-dihydro-1*H*-pyrrolizine-5-carboxamide (**5a**) was the most active analgesic agent. Cytotoxicity of the new compounds was evaluated against the MCF-7, A2780 and HT29 cancer cell lines using the MTT assay. Compounds **4b** and **5b** displayed high anticancer activity with IC_{50} in the range of 0.30–0.92 $\mu\text{mol L}^{-1}$ against the three cell lines, while compound (*EZ*)-*N*-(4-chlorophenyl)-7-cyano-6-((4-hydroxybenzylidene)-amino)-2,3-dihydro-1*H*-pyrrolizine-5-carboxamide (**4c**) was the most active against MCF-7 cells ($IC_{50} = 0.08 \mu\text{mol L}^{-1}$). Both the anti-inflammatory and anticancer activities of the new compounds were dependent on the type of substituent on the phenyl rings. Substituents with opposite electronic effects on the two phenyl rings are preferable for high cytotoxicity against the MCF-7 and A2780 cells. COX inhibition was suggested as the molecular mechanism of the anti-inflammatory activity of the new compounds while no clear relationship could be observed between COX inhibition and anticancer activity. Compound **5b**, the most active against the three cell lines, induced dose-dependent early apoptosis with 0.1–0.2 % necrosis in MCF-7 cells. New compounds showed promising drug-likeness scores while the docking study revealed high binding affinity to COX-2. Taken together, this study highlighted the significant impact of the substituents on the anti-inflammatory and anticancer activity of pyrrolizine-5-carboxamides, which could help in further optimization to discover good leads for the treatment of cancer and inflammation.

Accepted March 18, 2018
Published online April 11, 2018

Keywords: pyrrolizine-5-carboxamide, anticancer, anti-inflammatory, COXs, apoptosis, substituent electronic effect

* Correspondence; e-mail address: amsaid@uqu.edu.sa; ahmed.gouda@pharm.bsu.edu.eg

Cancer and inflammation are closely linked biological processes where many anti-inflammatory agents displaying anticancer activity have provided evidence for this tight correlation (1–4). The use of NSAIDs in prevention and treatment of cancer has been discussed in several reports. NSAIDs can restore normal apoptosis and inhibit angiogenesis in cancer cells (2). Moreover, the COX-2 enzyme plays an important role in cellular proliferation and apoptosis (4). The upregulation of COX-2 in benign and malignant cancers provided evidence for this role (5). In addition, several COX-2 inhibitors displayed potent anticancer activity mediated by the induction of apoptosis (6, 7).

Recently, several reports have focused on the anti-inflammatory and anticancer activities of the pyrrolizine derivatives (8–10). Licofelone (Fig. 1) is one of the derivatives that underwent a phase III clinical trial as an anti-inflammatory drug (11). Licofelone also displayed potent anticancer activity with an IC_{50} value of $5.5 \mu\text{mol L}^{-1}$ against the human breast MCF-7 cell line (12). Although licofelone acts as a dual COX/5-LOX inhibitor, Tavolari *et al.* (13, 14) have provided evidence that it induces apoptosis through the mitochondrial pathway instead of COX/5-LOX inhibition.

MR22388 is another pyrrolizine derivative that showed potent antiproliferative activity against the leukemia L1210 cell line with the IC_{50} value of 15 nmol L^{-1} (Fig. 1). The anticancer activity of MR22388 was mediated by the induction of apoptosis, inhibition of tubulin polymerization and inhibition of several kinases (15–17). Moreover, we have reported several pyrrolizine-5-carboxamide derivatives with potent anticancer activity against the MCF-7 and A549 cancer cell lines (9, 18). Anticancer activities of these pyrrolizines were associated with activation of caspase 3/7 enzymes, inhibition of COXs and induction of apoptosis (9, 18).

In this study, scaffold A was designed by bearing two phenyl rings (A and B) attached to the pyrrolizine nucleus *via* two atom spacers (Fig. 1). To evaluate the impact of electronic effects of the substituents on the two phenyl rings on the anti-inflammatory, anal-

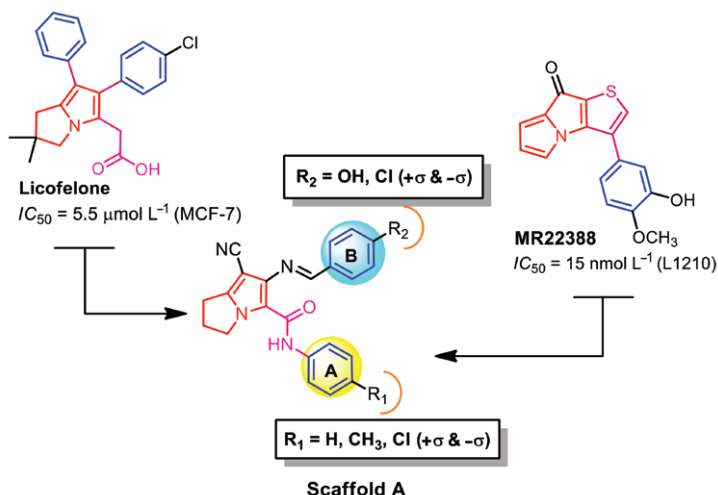


Fig. 1. Pyrrolizine-based anticancer agents and rational design of scaffold A.

gesic and anticancer activities of the new pyrrolizines, different types of substituents, including electron-donating groups (CH₃ and OH) and electron-withdrawing group (Cl), were used in the new compounds.

EXPERIMENTAL

Chemicals and instruments

All the chemical reagents and solvents used were purchased from Sigma-Aldrich (USA). Solvents were dried according to the literature when necessary. Purity of the new compounds was checked with TLC. Melting points are uncorrected and were determined with an IA 9100MK-Digital melting point apparatus (Cole-Parmer, USA). Infrared spectra (IR) were recorded using a BRUKER TENSOR 37 spectrophotometer (Bruker, USA) from KBr discs. The proton magnetic spectra were recorded on a BRUKER AVANCE III at 500 MHz (Bruker) in CDCl₃ and *J* constants were given in Hz. The ¹³C NMR and DEPT135 (distortionless enhancement by polarization transfer) spectra of the new compounds in CDCl₃ were done on the BRUKER AVANCE III (Bruker) at 125 MHz. Mass spectra were recorded using GCMS on a Shimadzu Qp-2010 Plus mass spectrometer (Shimadzu, Japan) at 70 eV (EI).

Syntheses

2-Pyrrolidin-2-ylidene-malononitrile (1). – Synthesis of 2-pyrrolidin-2-ylidene-malononitrile (**1**) was achieved according to previous reports (19). To a solution of 2-pyrrolidinone (2.5 g, 29.4 mmol) in dry benzene (30 mL), dimethyl sulfate (CH₃)₂SO₄ (3.7 g, 29.4 mmol) was added under stirring. The reaction mixture was refluxed for 3 hours and then allowed to cool to room temperature. The solution was cooled in an ice-bath and rendered alkaline by dropwise addition of sodium hydroxide (15 mol L⁻¹, 1.5 mL). The temperature was kept below 5 °C during the addition of sodium hydroxide. The organic phase was separated, dried over anhydrous sodium sulfate and filtered. Malononitrile (1.25 g, 19.1 mmol) was added to the benzene solution at room temperature. The produced solution was then stirred, whereby white crystals were formed on scratching the wall of the beaker. The crystals were collected, dried to give 5.2 g and recrystallized from aqueous ethanol.

2-Chloro-1N-[4-(un)substituted-phenyl]-acetamide (2a-c). – Synthesis of acetanilides **2a-c** was achieved according to a previous report (20) with some modifications. The appropriate aniline (27 mmol) was dissolved in a small amount of glacial acetic acid. Chloroacetyl chloride (4.55 g, 40.5 mmol) was added dropwise to the solution under continuous stirring and cooling. After addition of chloroacetyl chloride was completed, a saturated solution of sodium acetate (1.5 mL) was added dropwise under stirring. The solution was kept cool during the addition of chloroacetyl chloride by using an ice-cooled water-bath. The white precipitate formed was collected on a Büchner funnel, washed with water 2 times (2 × 30 mL) and recrystallized from aqueous ethanol. The following compounds were prepared: 2-chloro-*N*-phenylacetamide (**2a**), 2-chloro-*N*-(*p*-tolyl)acetamide (**2b**) and 2-chloro-*N*-(4-chlorophenyl)acetamide (**2c**).

Table I. Physicochemical data and mass spectra of new compounds **4a-c** and **5a-c**

Compd.	Yield (%)	M. p. (°C)	Molecular formula (M_r)	Elemental analysis (%)		MS (EI)
				Calcd.	Found	
4a	68	276–278	C ₂₂ H ₁₈ N ₄ O ₂ (370.40)	C: 71.34 H: 4.90 N: 15.13	C: 71.17 H: 5.39 N: 15.32	<i>m/z</i> (%) 373 (M ⁺ +3, 22), 372 (M ⁺ +2, 5), 371 (M ⁺ +1, 20), 370 (M ⁺ , 100), 369 (M ⁺ -1, 75), 298 (11), 77 (1)
4b	63	279–281	C ₂₃ H ₂₀ N ₄ O ₂ (384.43)	C: 71.86 H: 5.24 N: 14.57	C: 71.80 H: 4.83 N: 14.96	<i>m/z</i> (%) 388 (M ⁺ +4, 3), 370 (79), 280 (2), 279 (19), 278 (100), 277 (32), 266 (40), 250 (25), 174 (18), 92 (19), 77 (17)
4c	61	284–286	C ₂₂ H ₁₇ ClN ₄ O ₂ (404.85)	C: 65.27 H: 4.23 N: 13.84	C: 64.82 H: 4.58 N: 14.01	<i>m/z</i> (%) 407 (M ⁺ +3, 2), 406 (M ⁺ +2, 8), 405 (M ⁺ +1, 7), 404 (M ⁺ , 27), 403 (M ⁺ -1, 7), 370 (100), 278 (4)
5a	58	227–229	C ₂₂ H ₁₇ ClN ₄ O (388.85)	C: 67.95 H: 4.41 N: 14.41	C: 68.31 H: 4.87 N: 14.56	<i>m/z</i> (%) 391 (M ⁺ +3, 3), 390 (M ⁺ +2, 20), 389 (M ⁺ +1, 25), 388 (M ⁺ , 69), 370 (5), 296 (100), 277 (11), 77 (1)
5b	62	236–237	C ₂₃ H ₁₉ ClN ₄ O (402.88)	C: 68.57 H: 4.75 N: 13.91	C: 68.94 H: 5.14 N: 14.09	<i>m/z</i> (%) 405 (M ⁺ +3, 3), 404 (M ⁺ +2, 9), 403 (M ⁺ +1, 7), 402 (M ⁺ , 26), 401 (M ⁺ -1, 2), (370 (9), 296 (100), 268 (3), 77 (8)
5c	63	239–241	C ₂₂ H ₁₆ Cl ₂ N ₄ O (423.29)	C: 62.42 H: 3.81 N: 13.24	C: 62.31 H: 3.84 N: 13.28	<i>m/z</i> (%) 425 (M ⁺ +3, 8), 424 (M ⁺ +2, 20), 423 (M ⁺ +1, 6), 422 (M ⁺ , 28), 383 (27), 372 (37), 354 (21), 339 (16), 311 (22), 296 (100), 280 (19), 155 (2), 113 (3), 77 (2)

6-Amino-7-cyano-N-[4-(*un*)substituted-phenyl]-2,3-dihydro-1H-pyrrolizine-5-carboxamide (**3a-c**). – Synthesis of pyrrolizine-5-carboxamides **3a-c** was achieved according to a previous report (21). Appropriate acetanilides **2a-c** (7.5 mmol) were refluxed for 24 h with an equimolar ratio of 2-pyrrolidin-2-ylidene-malononitrile (**1**) in dry acetone in the presence of a catalytic amount of anhydrous potassium carbonate (0.5 g, 3.75 mmol). The mixture was filtered while hot, the content of the flask was washed 2 times with acetone (2 × 15 mL), left to cool and yellowish white crystals were separated. The following compounds were prepared: 6-amino-7-cyano-N-phenyl-2,3-dihydro-1H-pyrrolizine-5-carboxamide (**3a**), 6-amino-7-cyano-N-(*p*-tolyl)-2,3-dihydro-1H-pyrrolizine-5-carboxamide (**3b**) and 6-amino-N-(4-chlorophenyl)-7-cyano-2,3-dihydro-1H-pyrrolizine-5-carboxamide (**3c**).

(E)-7-cyano-6-((4-hydroxychlorobenzylidene)amino)-N-(*un*)substitutedphenyl-2,3-dihydro-1H-pyrrolizine-5-carboxamide (**4a-c** and **5a-c**). General procedures. – A mixture of the appropriate pyrrolizine-5-carboxamides **3a-c** (2 mmol) and appropriate aldehyde (2.2 mmol) in absolute ethanol (30 mL) in the presence of glacial acetic acid (0.5 mL) was refluxed for 6 hours.

The reaction mixture was then concentrated and set aside to cool. The yellow crystals formed were collected and recrystallized from chloroform-acetone (1:1). The following compounds were prepared: (*EZ*)-7-cyano-6-((4-hydroxybenzylidene)amino)-*N*-phenyl-2,3-dihydro-1*H*-pyrrolizine-5-carboxamide (**4a**), (*EZ*)-7-cyano-6-((4-hydroxybenzylidene)amino)-*N*-(*p*-tolyl)-2,3-dihydro-1*H*-pyrrolizine-5-carboxamide (**4b**), (*EZ*)-*N*-(4-chlorophenyl)-7-cyano-6-((4-hydroxybenzylidene)-amino)-2,3-dihydro-1*H*-pyrrolizine-5-carboxamide (**4c**), (*EZ*)-6-((4-chlorobenzylidene)amino)-7-cyano-*N*-phenyl-2,3-dihydro-1*H*-pyrrolizine-5-carboxamide (**5a**), (*EZ*)-6-((4-chlorobenzylidene)-amino)-7-cyano-*N*-(*p*-tolyl)-2,3-dihydro-1*H*-pyrrolizine-5-carboxamide (**5b**) and (*EZ*)-6-((4-chlorobenzylidene)amino)-*N*-(4-chlorophenyl)-7-cyano-2,3-dihydro-1*H*-pyrrolizine-5-carboxamide (**5c**).

Physicochemical properties and spectral data of the synthesized compounds are presented in Tables I and II.

Animals

The anti-inflammatory testing of the new compounds **4a-c** and **5a-c** was performed on adult albino rats (both sexes) weighing 100–140 g, while the analgesic activity was tested on albino mice of either sex (18–22 g). The animals were acquired from the animal house of King Abdul-Aziz University Medical Research Centre, Jeddah (Kingdom of Saudi Arabia). The animals were housed in polypropylene cages bedded with wooden husk. The animals were kept with food and tap water *ad libitum* and under a 12 h light/dark cycle).

Animals were divided into 8 groups of six animals each. Rats were hydrated orally with 3 mL water. Animals were kept in the lab for one week before starting the tests so as to adapt to lab conditions.

The animal ethical clearance was obtained from the Ethical Committee of the College of Pharmacy, Umm Al-Qura University, Makkah, KSA.

Pharmacological screening

Anti-inflammatory activity. – Carrageenan induced rat paw edema method was used for the anti-inflammatory activity evaluation according to a previous report (22). The control group was given saline solution containing a few drops of carboxy methyl cellulose (CMC) (group I). Ibuprofen (100 mg kg⁻¹, 0.48 mmol kg⁻¹ bm) prepared in distilled water containing a few drops of CMC was given to group II. Tested compounds **4a-c** and **5a-c** (0.48 mmol kg⁻¹ bm) suspended in distilled water containing a few drops of CMC were given to groups III-VIII.

Experimental procedures were performed following our previous report (10). Induction of inflammation was performed by a subcutaneous (*s.c.*) injection of 50 µL of 0.5 % carrageenan-sodium gel (Sigma-Aldrich, USA) into the sub-plantar region of the right hind paw. The dorsoventral diameter (thickness) of the right and left hind paws of each rat was measured using digital calipers with 0.01 mm accuracy (Cole-Parmer, USA). Edema thickness was measured 2 and 3 h after induction of inflammation. Results are presented in Table III.

In vivo analgesic activity. – Analgesic activity of the new compounds **4a-c** and **5a-c** was evaluated using the hot-plate test according to a previous report (23). The standard drug,

Table II. IR, ¹H NMR, ¹³C NMR and DEPT¹³⁵ spectra of new compounds 4a-c and 5a-c

Compd.	IR (ν, cm ⁻¹)	¹ H NMR (500 MHz, δ ppm)	¹³ C NMR (125 MHz, δ ppm)	DEPT ¹³⁵ (125 MHz, δ ppm)
4a	3216 (NH), 3074, 3029 (Ar C-H), 2953, 2903 (aliphatic C-H), 2211 (CN), 1669 (C=O), 1583 (C=C, C=N), 1313, 1275 (C-C, C-N, C-O)	(DMSO-d ₆): 2.51 (m, 2H, CH ₂ -2), 3.02 (t, 2H, J = 7.3 Hz, CH ₂ -1), 4.40 (t, 2H, J = 6.9 Hz, CH ₂ -3), 5.52 (s, H, OH), 6.97 (d, 2H, J = 8.0 Hz, aromatic CH-3' + CH-5'), 7.10 (t, H, J = 7.3 Hz, aromatic CH-4), 7.38 (t, 2H, J = 7.7 Hz, aromatic CH-3' + CH-5'), 7.64 (d, 2H, J = 7.9 Hz, aromatic CH-2' + CH-6'), 7.87 (d, 2H, J = 8.2 Hz, aromatic CH-2' + CH-6'), 8.91 (s, H, N=CH), 10.47 (s, H, CONH)	(DMSO-d ₆): 24.55, 25.50, 50.38, 76.59, 116.10, 116.44, 116.95, 117.33, 119.40, 124.05, 129.67, 129.87, 131.53, 138.77, 140.97, 149.01, 158.28, 161.00	(DMSO-d ₆): 24.55 (CH ₂ -2), 25.50 (CH ₂ -1), 50.38 (CH ₂ -3), 116.95 (aromatic CH-3' + CH-5'), 119.39 (aromatic CH-2' + CH-6'), 124.05 (aromatic CH-4), 129.67 (aromatic CH-3' + CH-5'), 131.54 (aromatic CH-2' + CH-6')
	3309 (NH), 3069, 3030 (Ar C-H), 2982, 2856 (aliphatic C-H), 2214 (CN), 1671 (C=O), 1604, 1582 (C=C, C=N), 1302, 1258 (C-C, C-N, C-O)	(CDCl ₃): 2.42 (s, 3H, CH ₃), 2.67 (m, 2H, CH ₂ -2), 3.12 (t, 2H, J = 7.4 Hz, CH ₂ -1), 4.36 (t, 2H, J = 6.9 Hz, CH ₂ -3), 5.49 (s, H, OH), 6.96 (d, 2H, J = 8.0 Hz, aromatic CH-3' + CH-5'), 7.15 (d, 2H, J = 7.6 Hz, aromatic CH-3' + CH-5'), 7.32 (d, 2H, J = 7.6 Hz, aromatic CH-2' + CH-6'), 7.83 (d, 2H, J = 8.0 Hz, aromatic CH-2' + CH-6'), 8.37 (s, H, N=CH), 9.90 (s, H, CONH)	(CDCl ₃): 21.42, 25.29, 26.16, 48.39, 116.02, 117.65, 122.90, 127.58, 128.31, 128.38, 130.35, 130.41, 132.47, 139.14, 141.18, 149.65, 152.03, 158.87, 161.18	(CDCl ₃): 21.42 (CH ₃), 25.29 (CH ₂ -2), 26.16 (CH ₂ -1), 48.39 (CH ₂ -3), 116.02 (aromatic CH-3' + CH-5'), 128.37 (aromatic CH-2' + CH-6'), 130.36 (aromatic CH-3' + CH-5'), 132.48 (aromatic CH-2' + CH-6')
4b	3324 (NH), 3063 (Ar C-H), 2986, 2900 (aliphatic C-H), 2212 (CN), 1668 (C=O), 1603, 1580 (C=C, C=N), 1307, 1278 (C-C, C-N, C-O), 812 (C-C)	(DMSO-d ₆): 2.50 (m, 2H, CH ₂ -2), 3.02 (t, 2H, J = 7.5 Hz, CH ₂ -1), 4.38 (t, 2H, J = 7.5 Hz, CH ₂ -3), 5.58 (s, H, OH), 6.98 (d, 2H, J = 6.5 Hz, aromatic CH-3' + CH-5'), 7.44 (d, 2H, J = 7.1 Hz, aromatic CH-3' + CH-5'), 7.66 (d, 2H, J = 7.2 Hz, aromatic CH-2' + CH-6'), 7.87 (d, 2H, J = 6.7 Hz, aromatic CH-2' + CH-6'), 8.91 (s, H, N=CH), 10.51 (s, H, CONH)	(DMSO-d ₆): 24.56, 25.47, 50.37, 76.66, 115.94, 116.38, 116.90, 121.04, 121.96, 127.55, 128.90, 129.51, 131.57, 137.68, 141.12, 149.19, 158.30, 161.10	(DMSO-d ₆): 24.57 (CH ₂ -2), 25.47 (CH ₂ -1), 50.36 (CH ₂ -3), 116.90 (aromatic CH-3' + CH-5'), 121.03 (aromatic CH-2' + CH-6'), 129.52 (aromatic CH-3' + CH-5'), 131.57 (aromatic CH-2' + CH-6')

5a	<p>3236 (NH), 3063, 3004 (Ar C-H), 2962, 2903 (aliphatic C-H), 2213 (CN), 1664 (C=O), 1597, 1550 (C=C, C=N), 1315, 1256 (C-C, C-N), 761 (C-Cl)</p>	<p>(CDCl₃): 2.58 (m, 2H, CH₂-2), 3.05 (t, 2H, J = 7.3 Hz, CH₂-1), 4.55 (t, 2H, J = 6.9 Hz, CH₂-3), 7.15 (t, H, J = 7.2 Hz, aromatic CH-4), 7.39 (t, 2H, J = 7.3 Hz, aromatic CH-3' + CH-5), 7.53 (d, 2H, J = 7.4 Hz, aromatic CH-3" + CH-5"), 7.65 (d, 2H, J = 7.7 Hz, aromatic CH-2' + CH-6'), 7.87 (d, 2H, J = 7.8 Hz, aromatic CH-2" + CH-6"), 9.14 (s, H, N=CH), 10.56 (s, H, CONH)</p>	<p>(CDCl₃): 24.54, 25.43, 50.21, 116.20, 118.08, 119.59, 124.09, 129.20, 129.56, 129.77, 130.93, 133.87, 138.19, 138.60, 138.78, 148.39, 158.24, 158.35 (aromatic CH-3' + CH-5'), 129.56 (aromatic CH-3" + CH-5"), 129.77 (aromatic CH-2' + CH-6"), 158.08 (N=CH)</p>
5b	<p>3234 (NH), 3073, 3030 (Ar C-H), 2954, 2923 (aliphatic C-H), 2213 (CN), 1662 (C=O), 1612, 1598 (C=C, C=N), 1316, 1299 (C-C, C-N), 837 (C-Cl)</p>	<p>(CDCl₃): 2.36 (s, 3H, CH₃), 2.55 (m, 2H, CH₂-2), 3.01 (t, 2H, J = 7.5 Hz, CH₂-1), 4.53 (t, 2H, J = 6.4 Hz, CH₂-3), 7.18 (d, 2H, J = 8.0 Hz, aromatic CH-3' + CH-5'), 7.51 (t, 4H, J = 7.5 Hz, aromatic CH-3" + CH-5" + CH-2' + CH-6'), 7.83 (d, 2H, J = 8.3 Hz, aromatic CH-2" + CH-6"), 9.11 (s, H, N=CH), 10.48 (s, H, CONH)</p>	<p>(CDCl₃): 20.92, 24.49, 25.41, 50.20, 116.26, 118.19, 119.51, 129.50, 129.67, 129.73, 130.93, 133.68, 133.87, 135.62, 138.50, 138.54, 148.31, 157.95, 158.19 (aromatic CH-2', 24.49 (CH₂-2), 25.41 (CH₂-1), 50.20 (CH₂-2), 119.50 (aromatic CH-2' + CH-6'), 129.50 (aromatic CH-3" + CH-5"), 129.68 (aromatic CH-3' + CH-5"), 129.73 (aromatic CH-2" + CH-6"), 157.93 (N=CH)</p>
5c	<p>3230 (NH), 3066 (Ar C-H), 2985, 2918 (aliphatic C-H), 2213 (CN), 1670 (C=O), 1595, 1547 (C=C, C=N), 1311, 1254 (C-C, C-N), 813 (C-Cl)</p>	<p>(CDCl₃): 2.60 (m, 2H, CH₂-2), 3.09 (t, 2H, J = 7.6 Hz, CH₂-1), 4.56 (t, 2H, J = 7.1 Hz, CH₂-3), 7.35 (d, 2H, J = 8.2 Hz, aromatic CH-3' + CH-5'), 7.55 (d, 2H, J = 7.8 Hz, aromatic CH-3" + CH-5"), 7.61 (d, 2H, J = 8.1 Hz, aromatic CH-2' + CH-6'), 7.88 (d, 2H, J = 7.8 Hz, aromatic CH-2" + CH-6"), 9.18 (s, H, N=CH), 10.61 (s, H, CONH)</p>	<p>(CDCl₃): 24.59 (CH₂-2), 25.44 (CH₂-1), 50.21 (CH₂-3), 120.74 (aromatic CH-2' + CH-6'), 129.19 (aromatic CH-3" + CH-5"), 129.63 (aromatic CH-3' + CH-5), 129.79 (aromatic CH-2" + CH-6"), 158.55 (N=CH)</p>

Table III. Anti-inflammatory and analgesic activities of compounds **4a-c** and **5a-c** and ibuprofen

Compd.	Anti-inflammatory activity ^a						Analgesic activity ^d								
	Change in edema thickness × 10 ⁻² (mm)			Inhibition of inflammation (%)			Potency ^b			MPE (%) ^c			Potency ^c		
	2 h	3 h	3 h	2 h	3 h	3 h	2 h	3 h	3 h	2 h	3 h	2 h	3 h	2 h	3 h
Control	0.415 ± 0.030	0.443 ± 0.042	–	–	–	–	–	–	–	–	–	–	–	–	–
4a	0.303 ± 0.034*	0.286 ± 0.026*	26.9	35.6	0.73	0.80	29.5 ± 1.8	39.8 ± 4.9 ^δ	0.74	0.77	–	–	–	–	–
4b	0.333 ± 0.024**	0.277 ± 0.013*	19.7	36.8	0.53	0.83	24.2 ± 3.7	37.4 ± 2.4 ^δ	0.61	0.72	–	–	–	–	–
4c	0.307 ± 0.032***	0.297 ± 0.031**	26.1	33.1	0.71	0.74	19.0 ± 1.6	35.2 ± 3.2 ^δ	0.48	0.68	–	–	–	–	–
5a	0.332 ± 0.035*	0.312 ± 0.025	20.1	29.7	0.54	0.67	29.4 ± 5.6	43.3 ± 3.9	0.74	0.84	–	–	–	–	–
5b	0.298 ± 0.025**	0.277 ± 0.014*	28.1	37.6	0.76	0.84	22.6 ± 2.6	40.1 ± 2.9 ^δ	0.57	0.77	–	–	–	–	–
5c	0.323 ± 0.047**	0.292 ± 0.041**	22.1	34.2	0.60	0.77	24.2 ± 2.1	30.6 ± 1.7 ^δ	0.61	0.59	–	–	–	–	–
Ibuprofen	0.262 ± 0.025	0.246 ± 0.018	37.05	44.6	1.00	1.00	39.8 ± 3.2	51.8 ± 2.5	1.00	1.00	–	–	–	–	–

^a Anti-inflammatory/analgesic activity was determined at a 0.48 mmol kg⁻¹ bm oral dose.

^b MPE – maximum protective effect; data expressed as mean ± SEM (*n* = 6). ^c Potency – anti-inflammatory/analgesic activity of tested compound divided by anti-inflammatory/analgesic activity of ibuprofen at the same time.

Statistically significant difference *vs.* ibuprofen: **p* < 0.05, ***p* < 0.001, ****p* < 0.0001; *vs.* control: ^δ*p* < 0.01.

ibuprofen (100 mg kg⁻¹ bm), and the test compounds (both 0.48 mmol kg⁻¹ bm) were given orally. Experimental procedures were performed following a previous report (10). Analgesic effect of the tested compounds was calculated as the percentage of the maximal protective effect. Results are presented in Table III.

In vitro COX-1/2 inhibition assay. – All new compounds (**4a-c** and **5a-c**) were tested for their inhibitory activity against both COX-1 (ovine) and COX-2 (human recombinant) enzymes. A COX inhibitor screening assay kit (Cayman Chemicals, USA) was used in the assay. The assay was done following the manufacturer's instructions and as mentioned before (24). The results were presented as % inhibition at a 10 μmol L⁻¹ concentration of the new compounds. Indomethacin and celecoxib were used as reference drugs. Results are presented in Table IV.

Growth inhibition

Cell cultures. – Human breast MCF-7, ovarian A2780 and colon HT29 cancer cell lines were obtained from the American Type Culture Collection (Manassas, VA, USA). All cells were cultured in Dulbecco's modified Eagle medium (DMEM) supplemented with 10 % fetal bovine serum (FBS, Gibco, USA) in a humidified incubator containing 5 % CO₂ at 37 °C.

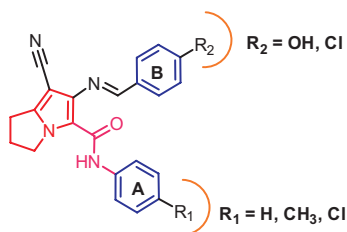
Cytotoxic activity. – The MTT (3-[4,5-dimethylthiazole-2-yl]-2,5-diphenyltetrazolium bromide, Merck, Germany) assay was used to investigate the anticancer activity of the new compounds following a previous report (25). Cells were seeded for 24 h (3 × 10³) in 96-well flat-bottomed plates. Seeded cells were then treated with the test compounds or lapatinib (*n* = 6). DMSO vehicle (0.1 %, V/V) was used as a negative control. Cells were treated with the tested compounds in final drug concentrations of 0.00, 0.05, 0.50, 5.00, 25.00 and 50.00 μmol L⁻¹. After 72 h, MTT was added for 3 h at 37 °C. Reduced MTT was dissolved in DMSO (100 μL per well). Absorbance was measured using a microplate reader at 570 nm and the

Table IV. *In vitro* inhibition of COX-1/2 enzymes by compounds **4a-c**, **5a-c** and reference drugs

Compd.	Inhibition (%) ^a	
	COX-1	COX-2
4a	28	42
4b	24	42
4c	31	48
5a	32	46
5b	31	40
5c	18	41
Indomethacin	72	63
Celecoxib	49	76

^a Inhibition of COX-1 (ovine) and COX-2 (human recombinant) at 10 μmol L⁻¹.

Table V. IC_{50} values of compounds **4a-c** and **2a-c** against MCF-7, A2780 and HT29 cancer cell lines



Compd.	R ₁	R ₂	IC_{50} ($\mu\text{mol L}^{-1}$)			
			MCF-7	A2780	HT29	Average value
4a	H	OH	0.31 ± 0.05	2.56 ± 0.29	0.96 ± 0.13	1.28
4b	CH ₃	OH	0.76 ± 0.60	0.92 ± 0.05	0.30 ± 0.16	0.67
4c	Cl	OH	0.08 ± 0.01	0.52 ± 0.02	3.79 ± 1.39	1.46
5a	H	Cl	1.12 ± 0.66	0.78 ± 0.30	0.37 ± 0.05	0.76
5b	CH ₃	Cl	0.33 ± 0.12	0.44 ± 0.01	0.41 ± 0.02	0.40
5c	Cl	Cl	1.77 ± 0.29	3.92 ± 0.07	0.72 ± 0.07	2.14
Lapatinib	–	–	6.80 ± 1.20	10.40 ± 0.80	12.67 ± 1.33	9.96

Results are mean \pm SD ($n = 6$ repetitive measurements, 3 independent experiments), after 72-h treatment with test compounds, lapatinib or 0.1 % DMSO (control).

readings were corrected by subtracting the negative control readings. Experiments were repeated three times independently. Results are represented in Table V.

Annexin V PI/FITC apoptosis assay. – Annexin V Propidium iodide/fluorescein isothiocyanate (PI/FITC) was used to evaluate the ability of compound **5b** to induce apoptotic changes in MCF-7 cells. Experimental procedures were done as previously reported (26). Three experiments were performed independently. Results are presented in Fig. 5.

Statistics

Anti-inflammatory and analgesic data were analyzed by One-way ANOVA followed by the Student-Newman-Keuls multiple comparison test.

Computational studies

Drug-likeness study. – Although a huge number of anticancer agents with potent activity *in vitro* have been reported in the last three decades, only a few have passed to clinical trials. This problem is mainly due to the ADME (absorption, distribution, metabolism and elimination) problems. In this work, the drug-likeness related parameters were deter-

Table VI. Molecular properties related to drug-likeness of compounds **4a-c**, **5a-c** and licofelone

Compd.	M_r	MV ^a	MR	TPSA	MlogP	RBs	H _A	H _D	LVs	DLS ^a
4a	370.4	382.82	108	90.41	1.6	5	4	2	0	0.55
4b	384.43	403.76	112.97	90.41	1.81	5	4	2	0	0.57
4c	404.85	400.01	113.01	90.41	2.08	5	4	2	0	1.00
5a	388.85	389.46	110.99	70.18	2.63	5	3	1	0	0.76
5b	402.88	410.40	115.95	70.18	2.84	5	3	1	0	0.81
5c	423.29	406.66	116	70.18	3.11	5	3	1	0	0.84
Licofelone	379.88	383.88	110.13	42.23	4.26	4	2	1	1 ^b	0.58

DLS – drug-likeness score, H_A – hydrogen bond acceptors, H_D – hydrogen bond donors, LVs – Lipinski violation, M_r – molecular mass, MV – molecular volume, TPSA – topological polar surface area, MlogP – Moriguchi's log P, RBs – rotatable bonds

^aParameters calculated using Molsoft: <http://molsoft.com/mprop/>; other parameters calculated using SwissADME (<http://www.swissadme.ch/>).

^bThere is one violation (MlogP > 4.15).

mined for the new compounds according to Lipinski's "rule of five" (27). The predicted values of the physicochemical properties of the new compounds were calculated using the SwissADME webserver developed by the Swiss Institute of Bioinformatics (SIB, Switzerland, <http://www.swissadme.ch/>) (28). Results are represented in Table VI.

The molecular mass (MW), molar refractivity (MR), lipophilicity (MlogP), number of hydrogen bond donors (H_D), number of hydrogen bond acceptors (H_A), Lipinski violations (27), number of rotatable bonds and topological polar surface area (TPSA) of the new compounds **4a-c** and **5a-c** and of licofelone were calculated. Chemical structures of the new compounds were sketched using the Marvin JS sketcher (version 16.4.18, 2016, www.chemaxon.com), converted to smiles by the JChem web service and processed through a series of actions when the calculation started upon clicking "RUN". The results were obtained as an Excel output file. The molecular volume and drug-likeness score (DLS) were calculated using the Molsoft webserver developed by Molsoft LLC (USA, <http://molsoft.com/mprop/>). The results are presented in Table VI.

Molecular docking study. – Docking study of all the new compounds was performed on COX enzymes. AutoDock 4.2 was used in the study and a Discovery Studio Visualizer (v16.1.0.15350) was used in visualization of the docking poses. Crystal structures of COX-1 (pdb code: 1EQG) (29) and COX-2 (pdb code: 1CX2) (30) were obtained from the protein data bank (<http://www.rcsb.org/pdb>). The protein structure was prepared by deleting water molecules and native ligands. Validation of the docking studies was done by re-docking the native ligands with their corresponding proteins. Binding modes and interactions of the native ligands with the key amino acids in the active site were identified and compared with the reported data.

Preparation of the protein (COX-1, COX-2) pdbqt files. – Crystal structures of the proteins co-crystallized with the native ligands were obtained from the Protein Data Bank (<http://www.rcsb.org/pdb>) as pdb files. COX-1 (pdb code: 1EQG) and COX-2 (pdb code: 1CX2) were obtained in X-ray resolution of 2.61 and 3.0 Å, resp. (29, 30). A discovery studio visualizer (DSV, v16.1.0.15350) was used to handle the protein structures. During preparation of the proteins, water molecules and bound ligands were removed to avoid interference with the study. The pdb files of the test compounds were prepared using Chem3D Ultra 8.0 followed by MOPAC energy minimization. The docking study was performed using AutoDock 4.2.

Preparation of ligand files. – Chemical structures of the new compounds were sketched using the ChemDraw Ultra 8.0 software. Chem3D Ultra 8.0 was used in the preparation of the ligand in the pdb format. Energies of the ligands were minimized using MOPAC with 100 iterations. The AutoDock Tool 1.5.6 was used to read the pdb files, add the hydrogens, compute Gasteiger charges, and to convert the pdb into the pdbqt format for the docking study. The docking scenario was done using flexible ligands while the rotatable bonds in the ligands were assigned using AutoDock tools (ADT) 1.5.6.

Preparation of affinity maps and running AutoGrid. – Preparation of the Grid parameter files by AutoDock was done using AutoGrid, which generated a map for each type of atom in the docking area. The 3D grids with the final size of 60 × 60 × 60 Å with 0.375 Å spacing were used in the study. The center of the grid for COX-1 was assigned at 26.643, 33.106 and 200.251 Å, and for COX-2 at 23.947, 21.582 and 15.436 Å.

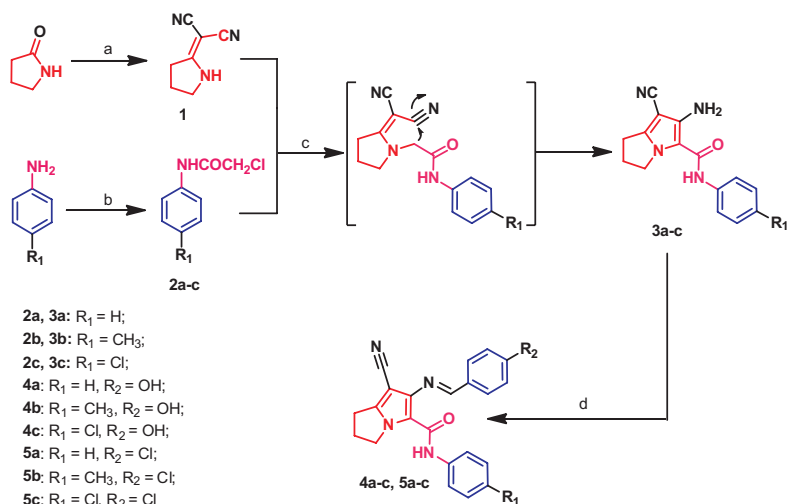
Preparation of the docking parameter file and running AutoDock. – The protein molecule and the ligand were selected to run AutoDock and perform docking calculations. The docking parameter file was set to the default values. In this study, we set the proteins as a rigid file while ligands were used as flexible molecules. Lamarckian genetic algorithm was set as the search parameter. After running AutoDock, the top ten conformations of the protein-ligand complex were clustered. Docking poses were scored and ranked in decreasing order of their binding free energy.

Analysis and visualization of the results. – AutoDock 4.2. was used in the analysis of the docking results, determination of the binding free energy (ΔG_b) and inhibition constants (K_i). Binding modes of the ligand and the type of ligand-protein interactions were visualized using a discovery studio visualizer (v16.1.0.15350). The 2D/3D binding mode was visualized showing both hydrogen bonding and hydrophobic interactions. The docking results are presented in Table VII and Figs. 6 and 7.

RESULTS AND DISCUSSION

Chemistry

Preparations of 2-pyrrolidin-2-ylidene-malononitrile (**1**), 2-chloro-1*N*-[4-(un)substituted-phenyl]-acetamides (**2a-c**) and 6-amino-7-cyano-*N*-[4-(un)substituted-phenyl]-2,3-dihydro-1*H*-pyrrolizine-5-carboxamides (**3a-c**) outlined in Scheme I were achieved following previous reports (19–21).



Reagents and reaction conditions: a) (CH₃)₂SO₄, benzene, malononitrile, b) ClCH₂COCl, glacial acetic acid, CH₃COONa, c) K₂CO₃, acetone, reflux, 24 h, d) appropriate aldehyde (4-hydroxy/4-chloro-benzaldehyde), ethanol, acetic acid, reflux, 6 h.

Scheme 1

Schiff bases **4a-c** and **5a-c** were obtained by the reaction of compounds **3a-c** with a proper aldehyde (4-hydroxybenzaldehyde or 4-chlorobenzaldehyde) in ethanol (see Scheme 1). Structural characterization of new compounds **4a-c** and **5a-c** was accomplished using IR, ¹H NMR, ¹³C NMR and mass spectra, in addition to elemental analyses (Tables I and II).

IR spectra of the new compounds **4a-c** and **5a-c** revealed absorption bands in the range of 3216–3324 cm⁻¹ indicating the NH of the amide groups, absorption bands in the range of 2211–2214 cm⁻¹ assigned to the cyano groups and stretching bands in the range of 1662–1671 cm⁻¹ attributed to the carbonyl groups.

¹H NMR spectra of compounds **4a-c** revealed three signals in the range of 2.50–4.56 ppm attributed to the aliphatic methylene groups of pyrrolizine nucleus. The ¹H NMR spectrum of compound **4b** revealed a singlet signal at 2.42 ppm assigned to the methyl group. A singlet signal in the range of 5.49–5.58 ppm was due to the protons of hydroxyl (OH) groups in compounds **4a-c**. Aromatic protons of compound **4a** appeared as two triplets at 7.10 and 7.38 ppm, in addition to three doublets at 6.97, 7.64 and 7.87 ppm, while the aromatic protons in compounds **4b** and **4c** appeared as four doublets in the range of 6.96–7.87 ppm. Two singlet signals were observed in the range of 8.37–10.51 ppm indicating benzylidene and amide protons, respectively. Superimposition of aromatic and amide protons in compound **4a** and in the intermediate compound (6-amino-7-cyano-*N*-phenyl-2,3-dihydro-1*H*-pyrrolizine-5-carboxamide) showed two new aromatic signals, in addition to a singlet signal of the benzylidene (N=CH) proton (Fig. 2).

The ¹H NMR spectrum of compound **5b** showed a singlet signal at 2.36 ppm due to the methyl group. Moreover, the ¹H NMR spectrum of compound **5a** revealed three signals in the

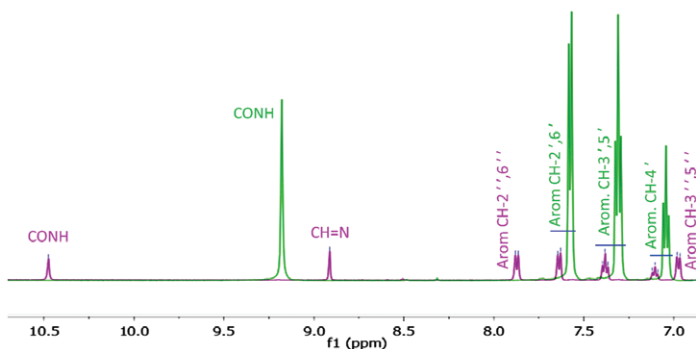


Fig. 2. Superimposition of the aromatic, benzyldene and amidic protons in compound **4a** (green) over the corresponding protons of compound **3a** (pink).

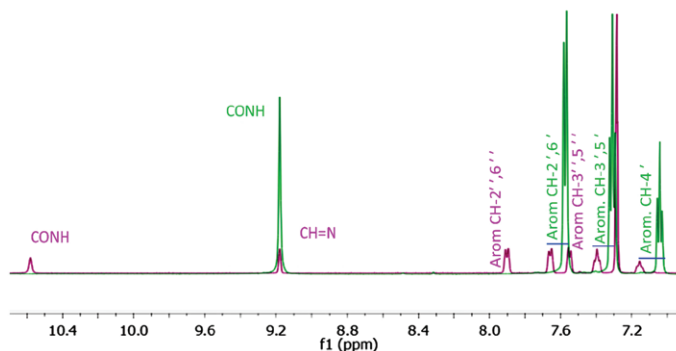


Fig. 3. Superimposition of the aromatic, benzyldene and amidic protons in compound **5a** (green) on the respective protons of compound **3a** (pink).

range of 2.55–4.56 ppm attributed to the methylene groups of the pyrrolidine ring. Aromatic protons of compound **5a** appeared as two triplets at 7.15 and 7.39 ppm plus three doublets at 7.53, 7.65 and 7.87 ppm, while the aromatic protons in compounds **5b** and **5c** appeared as four doublets in the range of 7.17–7.88 ppm indicating *para*-substituted phenyl rings. Two singlet signals at 8.91 and 10.47 ppm indicated benzyldene and amide protons, resp.

Superimposition of aromatic and amide protons in compound **5a** and the preceding compound **3a** showed two new aromatic signals, in addition to the benzyldene (N=CH) proton (Fig. 3).

On the other hand, the ^{13}C NMR spectra of compounds **4a-c** and **5a-c** revealed three signals in the range of 24.49–50.38 ppm attributed to the three aliphatic carbons of the pyrrolizine nucleus, two signals at 21.42 and 20.92 ppm attributed to the methyl (CH_3) groups in compounds **4b** and **5b**, resp. In addition, two signals in the range of 157.95–161.95 ppm were assigned to the benzyldene (C=NH) and carbonyl carbons in compounds **4a-c** and **5a-c**.

Pharmacological screening

In vivo anti-inflammatory activity. – Results of the anti-inflammatory activity are given as changes in edema thickness, inhibition of inflammation and relative potency compared to ibuprofen (Table III).

It was noticed that all new compounds showed moderate anti-inflammatory activity with relative potency in the range of 0.53–0.84 compared to ibuprofen. Ibuprofen and the new compounds (**4a-c** and **5a-c**) were significantly different from the control ($p = 0.001$).

Compounds **4a** and **5a** with the unsubstituted phenyl ring displayed anti-inflammatory activity of 35.6 and 29.7 %, resp. In general, the methyl-substituted analogs (**4b** and **5b**) displayed higher anti-inflammatory activity than the other derivatives (Table III).

In vivo analgesic activity. – Results from Table III revealed that all new compounds have analgesic activity lower than ibuprofen. Compounds **4a-c** with the 4-hydroxy substituent were less active than their 4-chloro analogs **5a-c**. Compound **5a** showed the highest analgesic activity after 3 hours (Table III).

In vitro COX-1/2 inhibitory activity. – New compounds **4a-c** and **5a-c** displayed inhibitory activity for COX-1/2 enzymes with inhibition in the range of 18–32 % for COX-1 and 41–48 % for COX-2 at $10 \mu\text{mol L}^{-1}$. Compound **4c** bearing 4-hydroxyphenyl was the most active COX-2 inhibitor while compound **5a** was the most active inhibitor of COX-1. All new compounds displayed inhibitory activity against COX-1 and COX-2 enzymes with inhibition lower than that of both the non-selective COX inhibitor (indomethacin) and the selective COX-2 inhibitor (celecoxib). All the inhibitions by the tested compounds were in the range of 18–48 % at 10 mmol L^{-1} , indicating that their IC_{50} values could be higher than 10 mmol L^{-1} (Table IV).

Anticancer activity

In vitro MTT assay. – New compounds showed cytotoxic activity against the three cell lines with IC_{50} values in the range of 0.08 to $3.92 \mu\text{mol L}^{-1}$, compared to lapatinib with IC_{50} of 6.80–12.67 $\mu\text{mol L}^{-1}$ (Table V). The 4-hydroxy derivatives **4a-c** displayed IC_{50} values in the range of 0.08–3.79 $\mu\text{mol L}^{-1}$ while the 4-chloro analogs **5a-c** were slightly less active ($\text{IC}_{50} = 0.33\text{--}3.92 \mu\text{mol L}^{-1}$) against the three cell lines. Compounds **4c**, **4b** and **5b** were the most active against the MCF-7, A2780 and HT29 cancer cell lines.

Structure activity relationship (SAR)

Compound **4a** displayed IC_{50} values of 0.31, 2.56 and $0.96 \mu\text{mol L}^{-1}$ against MCF-7, A2780 and HT29 cells, resp. Substitution on ring A with the electron donating methyl group increased activity against the A2780 and HT29 cells, while the 4-chloro substitution increased activity against the MCF-7 and A2780 cancer cell lines. Moreover, replacement of 4-hydroxy in compound **4a** with the chloro group (compound **5a**) resulted in an increase in activity against the A2780 and HT29 cell lines (Fig. 4).

The anticancer activity of compounds **5a-c** was dependent on the type of substituent on ring A. The 4-methyl substituent in compound **5b** increased the activity against both

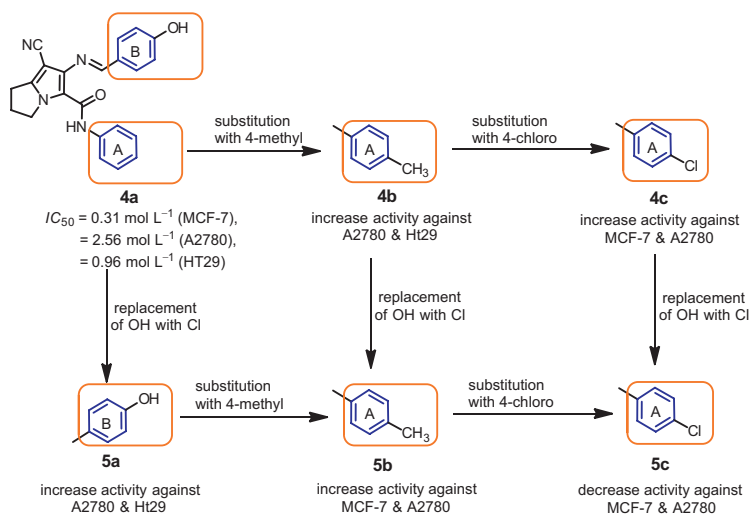


Fig. 4. SAR of the anticancer activity of the new compounds **4a-c** and **5a-c**.

MCF-7 and A2780 cells, while the 4-chloro decreased the activity against the three cell lines. On the other hand, replacement of the 4-hydroxy group in compound **4b** with the chloro group resulted in an increase of anticancer activity against both MCF-7 and A2780 cells, while replacement of the 4-hydroxy group in compound **4c** with the chloro group decreased the anticancer activity against both MCF-7 and A2780 cells.

In general, the electronic effect of various substituents on the anticancer activity varied with the cell line. Compound **4c** with the electron withdrawing Cl-group displayed higher activity against the MCF-7 and A2780 cell lines than compounds **4a** and **4b**, while the methyl derivative **5b** was more active than compounds **4a** and **4c** against these two cell lines. Accordingly, substituents on rings A and B of opposite electronic effects enhanced the anticancer activity against the MCF-7 and A2780 cell lines (Fig. 4).

Annexin V FITC/PI apoptosis assay

Annexin V propidium iodide(PI)/fluorescein isothiocyanate (FITC) apoptosis assay was used to evaluate the ability of the most active compound (**5b**) to induce apoptosis, following a previous report (26). The results are presented in Fig. 5. Compound **5b** induced dose dependent early apoptosis C4 (early apoptosis): 10.6, 32.4, 33.6 and 41.7 %, resp., for 0, 1, 5 and 10 $\mu\text{mol L}^{-1}$. Only 0.1–0.2 % necrosis (C1) was induced in the MCF-7 cell population by compound **5b**, following a 24-hour treatment. Compound **5b** caused at least four-fold increase in the early apoptotic events.

Computational study

Drug-likeness study. – The results revealed that the new compounds **4a-c** and **5a-c** have a molecular mass < 500, Moriguchi's lipophilicity (MlogP) lower than 5, hydrogen bond

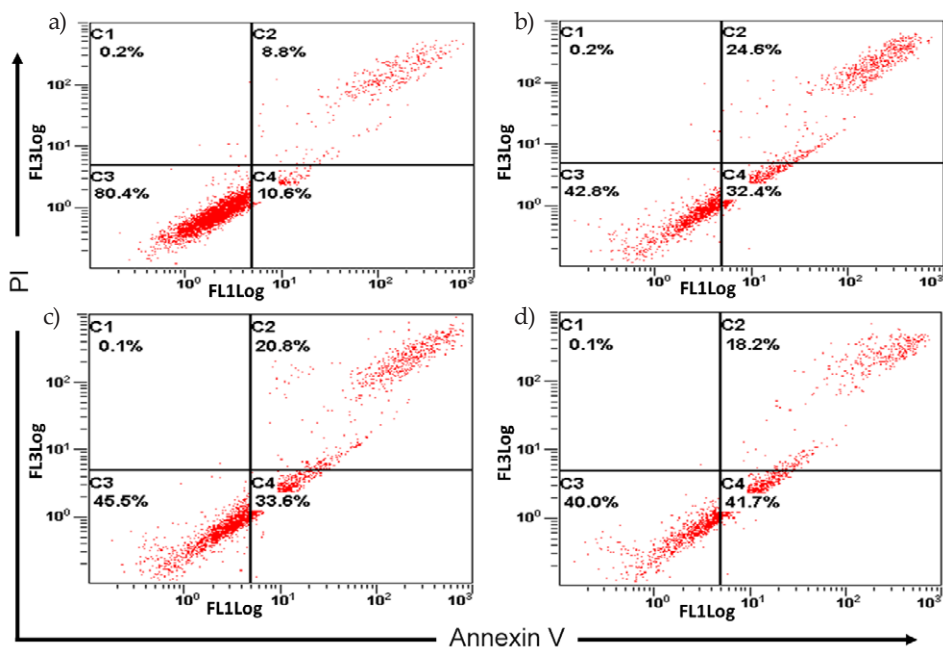


Fig. 5. Plots showing different phases of the staining of MCF-7 cells with annexin V FITC/PI, treated with compound **5b**, for 24 h: a) control, 0 $\mu\text{mol L}^{-1}$, b) 1 $\mu\text{mol L}^{-1}$, c) 5 $\mu\text{mol L}^{-1}$, d) 10 $\mu\text{mol L}^{-1}$ ($n = 3$).

x-axis: annexin V, y-axis: propidium iodide (PI)

C1: (necrosis-death, PI+/annexin V-); C2: (late apoptosis, PI+/annexin V+); C3: (living cells, PI-/annexin V-); C4: (early apoptosis, PI-/annexin V+).

acceptor (H_A) < 10, hydrogen bond donor (H_D) ≤ 5 , molar refractivity (MR) between 40 and 130. Accordingly, all the new compounds have good drug-likeness scores in the range of 0.55–1.00 compared to 0.58 for licofelone. No violation of Lipinski's rule was observed for the new compounds, while licofelone showed one violation (see Table V).

Docking study

Due to the important role of COXs enzymes in inflammation, cell proliferation and apoptosis (4–7), a comparative docking study was performed to evaluate the binding modes and binding free energies of the new compounds into the active sites of COX-1/2.

Docking study into the active site of COX-1. – COX-1 (ovine) crystal structure complexed with ibuprofen (pdb code: 1EQG) (29) was obtained from the protein data bank (<http://www.rcsb.org/pdb/home/home.do>). Validation of docking results was done by re-docking the native ligand (ibuprofen) into the active site of COX-1. A discovery studio visualizer (DSV) was used in visualization of the docking results. Docking results are presented in Table VII.

Results of the docking study revealed the ability of new compounds **4a-c** and **5a-c** to bind ARG120, TYR355, MET522 and SER530 amino acids in the active site of COX-1 with binding

Table VII. Results of the docking of compounds **4a-c** and **5a-c** into COX-1 in comparison with the native co-crystallized ligands^a

	Ligand	ΔG_b^b (kcal mol ⁻¹)	K_i^c ($\mu\text{mol L}^{-1}$)	No of HBs ^d	Atoms in H-bonding		Length (Å)
					In ligand	In protein	
COX-1	4a	-9.12	0.206	5	C $\underline{\text{O}}$ NH	N $\underline{\text{H}}$ of ARG120	2.17
					C $\underline{\text{O}}$ NH	N $\underline{\text{H}}$ of ARG120	2.74
					C $\underline{\text{O}}$ NH	O $\underline{\text{H}}$ of TYR355	2.18
					O $\underline{\text{H}}$	CO of MET522	2.22
					C $\underline{\text{N}}$	O $\underline{\text{H}}$ of SER530	2.24
	4b	-7.71	2.22	4	C $\underline{\text{O}}$ NH	N $\underline{\text{H}}$ of ARG120	2.43
					C $\underline{\text{O}}$ NH	N $\underline{\text{H}}$ of ARG120	2.86
					C $\underline{\text{O}}$ NH	O $\underline{\text{H}}$ of TYR355	2.98
					C $\underline{\text{N}}$	O $\underline{\text{H}}$ of SER530	2.52
	4c	-8.08	1.19	2	C $\underline{\text{O}}$ NH	O $\underline{\text{H}}$ of TYR355	3.13
					C $\underline{\text{O}}$ NH	N $\underline{\text{H}}$ of ARG120	3.14
	5a	-8.68	0.432	2	C $\underline{\text{O}}$ NH	NH ₂ of ARG120	1.55
					C $\underline{\text{O}}$ NH	N $\underline{\text{H}}$ of ARG120	2.61
	5b	-8.73	0.401	1	CH= $\underline{\text{N}}$	O $\underline{\text{H}}$ of TYR355	2.95
5c	-8.99	0.259	2	C $\underline{\text{O}}$ NH	NH ₂ of ARG120	2.04	
				C $\underline{\text{O}}$ NH	O $\underline{\text{H}}$ of TYR355	2.15	
Ibu.	-7.85	1.75	3	COOH	NH of ARG120	1.74	
				C=O	NH ₂ of ARG120	1.84	
				C=O	OH of TYR355	1.89	
COX-2	4a	-10.33	0.026	- ^e	-	-	-
	4b	-10.88	0.011	- ^e	-	-	-
	4c	-11.13	0.0069	- ^e	-	-	-
	5a	-10.05	0.04265	1	C $\underline{\text{O}}$ NH	NH ₂ of ARG120	2.83
	5b	-10.59	0.01732	1	C $\underline{\text{O}}$ NH	NH ₂ of ARG120	2.89
	5c	-10.88	0.01061	1	C $\underline{\text{O}}$ NH	NH ₂ of ARG120	3.10
	Sc-588	-10.78	0.01252	4	O of SO ₂	NH of HIS90	2.03
					H ¹ of NH ₂	CO of LEU352	2.08
H ² of NH ₂					CO of GLN192	1.97	
CF ₃					NH of ARG120	2.24	

^a COX-1 (pdb: 1eqg) (ref. 29) and COX-2 (pdb: 1cx2) (ref. 30).

^b Binding free energy.

^c Inhibition constant.

^d HBs - hydrogen bonds.

^e No hydrogen bond detected.

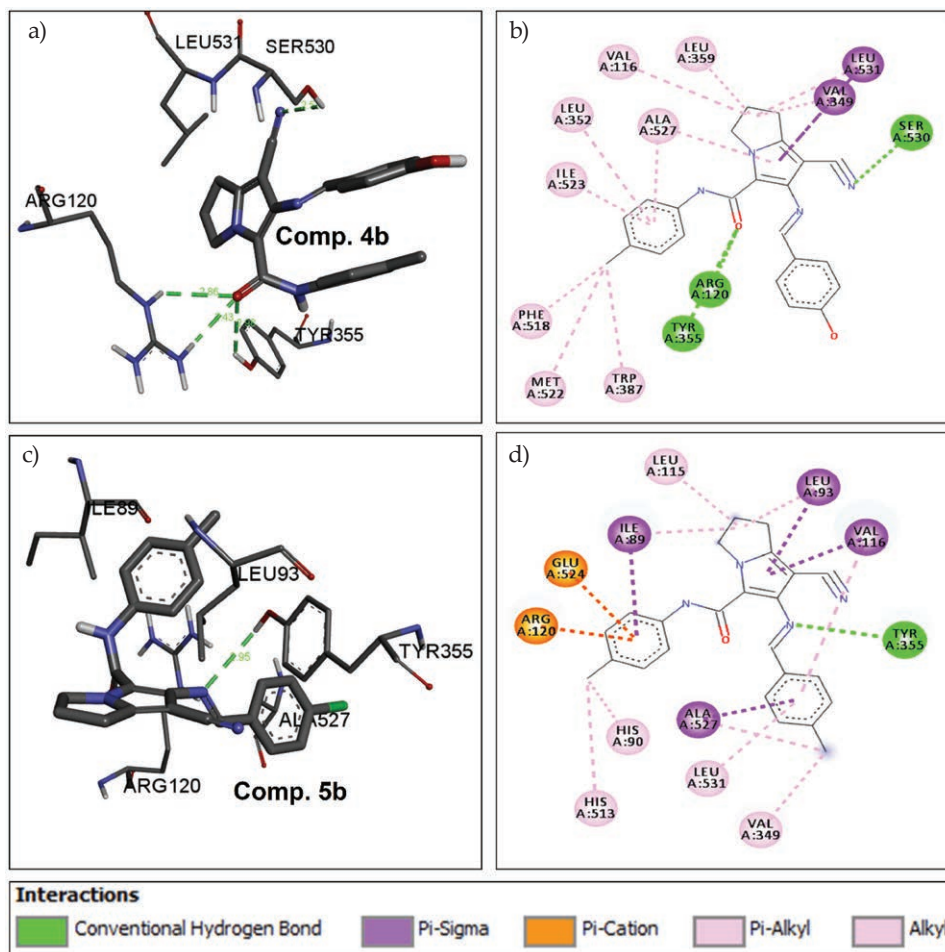


Fig. 6. a) 3D docking mode of compound **4b** into COX-1 (pdb code: 1EQG) showing four hydrogen bonds with ARG120, TYR355 and SER530 amino acids, b) 2D docking mode of compound **4b** into COX-1 showing four hydrogen bonds, twelve hydrophobic interactions of the pi-sigma, alkyl and pi-alkyl types, c) 3D docking mode of compound **5b** into COX-1 (pdb code: 1EQG) showing one hydrogen bond with TYR355, d) 2D docking mode of compound **5b** into COX-1 showing one hydrogen bond and fifteen hydrophobic interactions of the pi-cation, pi-sigma, alkyl and pi-alkyl types.

free energy in the range of -7.71 to -9.12 kcal mol $^{-1}$. Except for compound **4b**, all the new compounds showed binding affinity higher than ibuprofen ($\Delta G_b = -7.85$ kcal mol $^{-1}$). In addition, all the new compounds formed 1–5 hydrogen bonds with the amino acids in COX-1 (Table VII and Fig. 6).

Docking into the active site of COX-2. – New compounds were also docked into the active site of COX-2 using AutoDock 4.2. The crystal structure of COX-2 (pdb code: 1CX2) (30) was

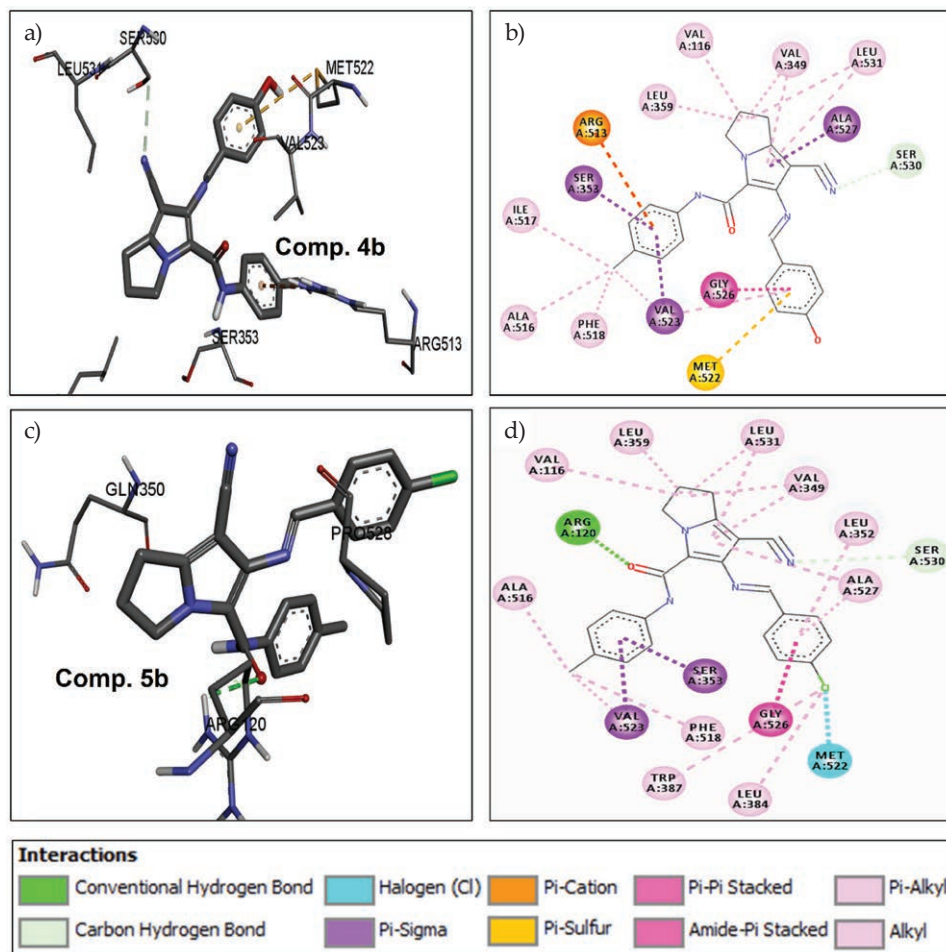


Fig. 7. a) 3D docking mode of compound **4b** into COX-2 (pdb code: 1CX2), b) 2D docking mode of compound **4b** into COX-2 showing eighteen hydrophobic interactions of the halogen (Cl), pi-cation, pi-sulfur, pi-sigma, amide-pi stacked, alkyl and pi-alkyl types, c) 3D docking mode of compound **5b** into COX-2 (pdb code: 1CX2) showing one hydrogen bond with ARG120, d) 2D docking mode of compound **5b** into COX-2 showing one hydrogen bond, nineteen hydrophobic interactions of the carbon-hydrogen, halogen (Cl), pi-sigma, amide-pi stacked, alkyl and pi-alkyl types.

obtained from the protein data bank (<http://www.rcsb.org/pdb/home/home.do>). Validation of docking results was done through a re-docking scenario of the native ligand (SC-558) into the active site of the COX-2 enzyme. New compounds displayed binding affinities comparable to or slightly higher than the native ligand SC-558 (Table VII). Hydrophobic interaction was the main type of interaction between the new compounds and amino acids in the active site of the enzyme. Although compounds **5a-c** showed only one hydrogen bonding with ARG120 in COX-2, their high binding affinities to COX-2 were mainly due to

the formation of multiple hydrophobic interactions (Fig. 7). To sum up, compounds **4c** and **5c** with the 4-chloro substitution on ring A displayed higher binding affinity to COX-2 than their methyl (**4b** and **5b**) and unsubstituted analogs (**4a** and **5a**).

CONCLUSIONS

A novel series of pyrrolizine-5-carboxamides derivatives **4a-c** and **5a-c** was prepared and evaluated for their anti-inflammatory, analgesic and anticancer activities. (*EZ*)-7-cyano-6-((4-hydroxybenzylidene)amino)-*N*-(*p*-tolyl)-2,3-dihydro-1*H*-pyrrolizine-5-carboxamide (**4b**) and (*EZ*)-6-((4-chlorobenzylidene)-amino)-7-cyano-*N*-(*p*-tolyl)-2,3-dihydro-1*H*-pyrrolizine-5-carboxamide (**5b**) bearing the electron donating methyl group showed the highest anti-inflammatory activity 3 hours after induction of inflammation, while (*EZ*)-7-cyano-6-((4-hydroxybenzylidene)amino)-*N*-phenyl-2,3-dihydro-1*H*-pyrrolizine-5-carboxamide (**4a**) and (*EZ*)-6-((4-chlorobenzylidene)amino)-7-cyano-*N*-phenyl-2,3-dihydro-1*H*-pyrrolizine-5-carboxamide (**5a**) were the most active analgesic agents.

Cytotoxicity of the new compounds was evaluated against the MCF-7, A2780 and HT29 cancer cell lines where the results revealed high anticancer activity. Substituents with opposite electronic effects on the two phenyl rings enhanced the anticancer activity against the MCF-7 and A2780 cell lines. (*EZ*)-*N*-(4-chlorophenyl)-7-cyano-6-((4-hydroxybenzylidene)-amino)-2,3-dihydro-1*H*-pyrrolizine-5-carboxamide (**4c**) displayed the highest anticancer activity against the MCF-7 and A2780 cell lines with IC_{50} values of 0.08 and 0.52 $\mu\text{mol L}^{-1}$, resp. COX inhibition was suggested as the possible mechanism of action of the anti-inflammatory activity of the new compounds. Results of the COX-1/2 inhibition assay showed appreciable inhibitory activity with higher inhibitory activity of COX-2. Although compound **4c** with the highest inhibition of COX-2 displayed the highest anticancer activity against the MCF-7 and A2780 cell lines, it was the least active against COX-2 producing HT29 cells. In addition, compound **5b** which displayed the lowest inhibition of COX-2 was the most active against the three cancer cell lines. These findings suggest that targets other than COX enzymes mediate the anticancer activity of these compounds. Annexin V PI/FITC apoptosis assay revealed the ability of compound **5b** to induce dose-dependent early apoptosis with 0.1–0.2 % necrosis in MCF-7 cells.

The drug-likeness study showed promising bioactivity scores for the new compounds. The docking study of the new compounds into COX-1/2 revealed high binding affinities for COX-2. Taken together, this study has confirmed the significant impact of different substituents on the biological activity of pyrrolizine-5-carboxamides, which could help in further optimization to discover good leads for the treatment of cancer and inflammation.

Acknowledgements. – The authors thank the Deanship of Scientific Research at the Umm Al-Qura University for their continuous support. This work was supported financially by the Deanship of Scientific Research of the Umm Al-Qura University, Makkah, Kingdom of Saudi Arabia, to Dr. Ahmed Mahmoud Gouda Said (Grant Code: 15-MED-3-1-0059).

Supplementary data are available upon request.

REFERENCES

1. E. R. Rayburn, S. J. Ezell and R. Zhang, Anti-inflammatory agents for cancer therapy, *Mol. Cell. Pharmacol.* **1** (2009) 29–43; <https://doi.org/10.4255/mcpharmacol.09.05>

2. M. J. Thun, S. J. Henley and C. Patrono, Nonsteroidal anti-inflammatory drugs as anticancer agents: mechanistic, pharmacologic, and clinical issues, *J. Natl. Cancer Inst.* **94** (2002) 252–266; <https://doi.org/10.1093/jnci/94.4.252>
3. S. R. Pedada, N. S. Yarla, P. J. Tambade, B. L. Dhananjaya, A. Bishayee, K. M. Arunasree, G. H. Philip, G. Dharmapuri, G. Aliev, S. Putta and G. Rangaiah, Synthesis of new secretory phospholipase A2-inhibitory indole containing isoxazole derivatives as anti-inflammatory and anticancer agents, *Eur. J. Med. Chem.* **112** (2016) 289–297; <https://doi.org/10.1016/j.ejmech.2016.02.025>
4. C. Sobolewski, C. Cerella, M. Dicato, L. Ghibelli and M. Diederich, The role of cyclooxygenase-2 in cell proliferation and cell death in human malignancies, *Int. J. Cell Biol.* **2010** (2010) 1–21; <https://doi.org/10.1155/2010/215158>
5. C. S. Williams, M. Mann and R. N. DuBois, The role of cyclooxygenases in inflammation, cancer, and development, *Oncogene* **18** (1999) 7908–7916; <https://doi.org/10.1038/sj.onc.1203286>
6. C. Ruegg, J. Zaric and R. Stupp, Non-steroidal anti-inflammatory drugs and COX-2 inhibitors as anti-cancer therapeutics: hypes, hopes and reality, *Ann. Med.* **35** (2003) 476–487; <https://doi.org/10.1080/07853890310017053>
7. A. T. Koki and J. L. Masferrer, Celecoxib: a specific COX-2 inhibitor with anticancer properties, *Cancer Control* **9** (2002) 28–35; <https://doi.org/10.1177/107327480200902S04>
8. A. M. Gouda and A. H. Abdelazeem, An integrated overview on pyrrolizines as potential anti-inflammatory, analgesic and antipyretic agents, *Eur. J. Med. Chem.* **114** (2016) 257–292; <https://doi.org/10.1016/j.ejmech.2016.01.055>
9. A. M. Gouda, A. H. Abdelazeem, H. A. Omar, A. N. Abdalla, M. A. S. Abourehab and H. I. Ali, Pyrrolizines: design, synthesis, anticancer evaluation and investigation of the potential mechanism of action, *Bioorg. Med. Chem.* **25** (2017) 5637–5651; <https://doi.org/10.1016/j.bmc.2017.08.039> (in press)
10. A. M. Gouda, H. I. Ali, W. H. Almalki, M. A. Azim, M. A. S. Abourehab and A. H. Abdelazeem, Design, synthesis, and biological evaluation of some novel pyrrolizine derivatives as COX inhibitors with anti-inflammatory/analgesic activities and low ulcerogenic liability, *Molecules* **21** (2016) 1–21; <https://doi.org/10.3390/molecules21020201>
11. J.-P. Raynaud, J. Martel-Pelletier, P. Bias, S. Laufer, B. Haraoui, D. Choquette, A. D. Beaulieu, F. Abram, M. Dorais, E. Vignon and J.-P. Pelletier, Protective effects of licofelone, a 5-lipoxygenase and cyclo-oxygenase inhibitor, versus naproxen on cartilage loss in knee osteoarthritis: a first multicentre clinical trial using quantitative MRI, *Ann. Rheum. Dis.* **68** (2009) 938–947; <https://doi.org/10.1136/ard.2008.088732>
12. W. Liu, J. Zhou, K. Bendorf, H. Zhang, H. Liu, Y. Wang, H. Qian, Y. Zhang, A. Wellner, G. Rubner, W. Huang, C. Guo and R. Gust, Investigations on cytotoxicity and anti-inflammatory potency of licofelone derivatives, *Eur. J. Med. Chem.* **46** (2011) 907–913; <https://doi.org/10.1016/j.ejmech.2011.01.002>
13. S. Tavorari, M. Bonafe, M. Marini, C. Ferreri, G. Bartolini, E. Brighenti, S. Manara, V. Tomasi, S. Laufer and T. Guarnieri, Licofelone, a dual COX/5-LOX inhibitor, induces apoptosis in HCA-7 colon cancer cells through the mitochondrial pathway independently from its ability to affect the arachidonic acid cascade, *Carcinogenesis* **29** (2008) 371–380; <https://doi.org/10.1093/carcin/bgm265>
14. S. Tavorari, A. Munarini, G. Storci, S. Laufer, P. Chieco and T. Guarnieri, The decrease of cell membrane fluidity by the non-steroidal anti-inflammatory drug Licofelone inhibits epidermal growth factor receptor signalling and triggers apoptosis in HCA-7 colon cancer cells, *Cancer Lett.* **321** (2012) 187–194; <https://doi.org/10.1016/j.canlet.2012.02.003>
15. V. Lisowski, C. Enguehard, J. Lancelot, D. Caignard, S. Lambel, S. Leonce, A. Pierre, G. Atassi, P. Renard and S. Rault, Design, synthesis and antiproliferative activity of tripentones: a new series of antitubulin agents, *Bioorg. Med. Chem. Lett.* **11** (2001) 2205–2208; [https://doi.org/10.1016/S0960-894X\(01\)00403-6](https://doi.org/10.1016/S0960-894X(01)00403-6)

16. V. Lisowski, S. Leonce, L. Kraus-Berthier, J. Sopkova-de Oliveira Santos, A. Pierre, G. Atassi, D.-H. Caignard, P. Renard and S. Rault, Design, synthesis, and evaluation of novel thienopyrrolizinones as antitubulin agents, *J. Med. Chem.* **47** (2004) 1448–1464; <https://doi.org/10.1021/jm030961z>
17. C. Rochais, T. Cresteil, V. Perri, M. Jouanne, A. Lesnard, S. Rault and P. Dallemagne, MR22388, a novel anti-cancer agent with a strong FLT-3 ITD kinase affinity, *Cancer Lett.* **331** (2013) 92–98; <https://doi.org/10.1016/j.canlet.2012.12.017>
18. A. M. Gouda, A. H. Abdelazeem, E.-S. A. Arafa and K. R. A. Abdellatif, Design, synthesis and pharmacological evaluation of novel pyrrolizine derivatives as potential anticancer agents, *Bioorg. Chem.* **53** (2014) 1–7; <https://doi.org/10.1016/j.bioorg.2014.01.001>
19. A. Etienne and Y. Correia, Derivatives of 2-pyrrolidone, *Bull. Soc. Chem.* **10** (1969) 3704–3712.
20. W. A. Jacobs and M. Heideberger, The ferrous sulfate and ammonia method for the reduction of nitro to amino compounds, *J. Am. Chem. Soc.* **39** (1917) 1435–1439; <https://doi.org/10.1021/ja02252a017>
21. M. Y. Ebeid, S. M. El-Moghazy, M. M. Hanna, F. A. Romeih and F. F. Barsoum, Synthesis and anti-HIV activity of some 6,7-dihydro-5H-pyrrolizine-3-carboxamide, 5,6,7,8-tetrahydroindolizine-3-carboxamide, 1-thioxo-1,2,3,5,6,7,8,9,10,11-decahydro-pyrimido-[1,6-*a*]azonine-4-carbonitrile and 6-thioxo-1,2,5,6,8,9,10,11,12,13,14,14a-dodecahydro-pyrimido[4,5':4,5]pyrimido-[1,6-*a*]azonine-1-one derivatives, *Bull. Fac. Pharm. Cairo Univ.* **35** (1997) 171–183.
22. C. A. Winter, E. A. Riskey and G. W. Nuss, Carrageenan induced edema in hind paw of the rats as an assay for anti-inflammatory drugs, *Proc. Soc. Exp. Biol. Med.* **111** (1962) 544–547; <https://doi.org/10.3181/00379727-111-27849>
23. A. Mollica, R. Costante, A. Stefanucci, F. Pinnen, G. Lucente, S. Fidanza and S. Pieretti, Novel cyclic biphalin analogue with improved antinociceptive properties, *J. Pept. Sci.* **19** (2013) 233–239; <https://pubs.acs.org/doi/10.1021/ml500241n>
24. N. Handler, W. Jaeger, H. Puschacher, K. Leisser and T. Erker, Synthesis of novel curcumin analogues and their evaluation as selective cyclooxygenase-1 (COX-1) inhibitors, *Chem. Pharm. Bull. (Tokyo)* **55** (2007) 64–71; <https://doi.org/10.1248/cpb.55.64>
25. E.-S. A. Arafa, A. H. Abdelazeem, H. H. Arab and H. A. Omar, OSU-CG5, a novel energy restriction mimetic agent, targets human colorectal cancer cells in vitro, *Acta Pharmacol. Sin.* **35** (2014) 394–400; <https://doi.org/10.1038/aps.2013.183>
26. I. Vermes, C. Haanen, H. Steffens-Nakken and C. Reutellingsperger, A novel assay for apoptosis. Flow cytometric detection of phosphatidylserine expression on early apoptotic cells using fluorescein labelled Annexin V, *J. Immunol. Methods* **184** (1995) 39–51; [https://doi.org/10.1016/0022-1759\(95\)00072-1](https://doi.org/10.1016/0022-1759(95)00072-1)
27. C. A. Lipinski, F. Lombardo, B. W. Dominy and P. J. Feeney, Experimental and computational approaches to estimate solubility and permeability in drug discovery and development settings, *Adv. Drug Deliv. Rev.* **23** (1997) 3–25; [https://doi.org/10.1016/S0169-409X\(96\)00423-1](https://doi.org/10.1016/S0169-409X(96)00423-1)
28. A. Daina, O. Michielin and V. Zoete, SwissADME: a free web tool to evaluate pharmacokinetics, drug-likeness and medicinal chemistry friendliness of small molecules, *Sci. Rep.* **7** (2017) Article ID 42717; <https://doi.org/10.1038/srep42717>
29. B. S. Selinsky, K. Gupta, C. T. Sharkey and P. J. Loll, Structural analysis of NSAID binding by prostaglandin H2 synthase: time-dependent and time-independent inhibitors elicit identical enzyme conformations, *Biochemistry* **40** (2001) 5172–5180; <https://doi.org/10.1021/bi010045s>
30. R. G. Kurumbail, A. M. Stevens, J. K. Gierse, J. J. McDonald, R. A. Stegeman, J. Y. Pak, D. Gildehaus, J. M. Miyashiro, T. D. Penning, K. Seibert, P. C. Isakson and W. C. Stallings, Structural basis for selective inhibition of cyclooxygenase-2 by anti-inflammatory agents, *Nature* **384** (1996) 644–648; <https://doi.org/10.1038/384644a0>